Buried Interface Molecular Hybrid Enables Efficient Perovskite Solar Cells

Tianyu Huang(黄天宇)[1], Rui Zhu(朱瑞)[1], and Deying Luo (罗德映)[2*]

[1]*State Key Laboratory for Artificial Microstructure and Mesoscopic Physics, School of Physics, Frontiers Science Center for Nano-optoelectronics & Collaborative Innovation Center of Quantum Matter, Peking University, Beijing 100871, China*
[2]*Department of Chemical and Nano Engineering, University of California San Diego, La Jolla, CA, USA*

(Received 22 July 2024; accepted manuscript online 13 August 2024)

DOI: 10.1088/0256-307X/41/9/098501

Perovskite solar cells (PSCs) with a positive-intrinsic-negative (p–i–n, commonly referred to as "inverted") structure are becoming commercially attractive due to their superior power conversion efficiency (PCE) and better operational stability as compared to the "normal" structure device.[1–5] Nonetheless, further improvements in the device performance of inverted PSCs are hampered by interface losses, particularly where the buried interfaces are responsible for perovskite crystallization and charge-carrier extraction.[6–9] In the context, the p-type hole charge-carrier extraction layer, which is deposited on top of the semitransparent electrodes (for example, indium tin oxide), must be able to minimize the non-radiative recombination at the buried interface, leveraging better wettability and charge-carrier extraction capability. Therefore, efforts to engineer the buried interface have been a focal point for the development of higher device-performance inverted PSCs.[10–14]

Since 2020, self-assembled monolayer (SAM) materials have been intensively investigated as the hole charge-carrier extraction layer in inverted PSCs, significantly advancing this technology.[11,15] Despite notable advances in device performance, the relatively poor wettability of SAM materials is considered as a major obstacle to pushing device performance towards the theoretical thermodynamic limit. In particular, when high-concentration perovskite precursor solutions are used to create micron-thick perovskite absorber layers on substrates with SAMs, the quality of the perovskite absorber thin films can be significantly reduced. Addressing the relatively poor wettability of SAM materials without compromising their charge-carrier extraction capability is a step forward in advancing inverted PSCs, including both tandem and single-junction solar cells.

Most recently, Liu *et al.* have demonstrated that co-assembling a multiple carboxylic acid functionalized aromatic compound, 4,4',4"-nitrilotribenzoic acid (NA), with commonly used SAM materials can address the long-standing challenges mentioned above.[12] The molecular structures used in their work are displayed in Fig. 1(a). Owing to the improved wettability with the molecular hybrid, the nanoscale voids introduced by the poor wettability of the single SAM layer can be eliminated when making the perovskite absorber thin film [as shown in Fig. 1(b)]. Grazing-incidence wide-angle x-ray scattering (GIWAXS) patterns reveal that the resulting perovskite absorber thin films exhibit improved crystallization intensities compared to regular ones [Fig. 1(c)], with reduced residual tensile stress that benefits device longevity [Fig. 1(d)]. Furthermore, laser confocal fluorescence lifetime imaging microscopy results indicate that the molecular hybrid can significantly improve the uniformity of the perovskite bottom surface, thereby reducing non-radiative recombination losses at the buried interface. This notable improvement in optoelectronic properties is verified by estimating the quasi-Fermi level splitting (QFLS) using photoluminescence quantum yield (PLQY) data [Fig. 1(e)].

Thanks to the quality of the buried interfaces and the corresponding perovskite absorber thin films, inverted PSCs with the molecular hybrid have achieved a record power conversion efficiency (PCE) of 26.54%, which is a record-certified steady-state efficiency [as shown in Figs. 1(f) and 1(g)].

More importantly, this molecular hybrid strategy is compatible with large-scale manufacturing, achieving a certified PCE of 22.74% for inverted mini-modules with an aperture area of 11.1 cm^2. In addition to device efficiency, the improved PSCs maintained 96.1% of their initial PCE after more than 2400 h of 1-sun operation in ambient air, in compliance with the IEC61215:2016 standard [as depicted in Figs. 1(h) and 1(i)]. These remarkable device performances fully indicate that the molecular hybrid strategy for engineering the buried interface is promising for development of efficient and stable PSCs. Following the same logic flow as mentioned above, it is conceivable that combining different functional molecules could improve the buried interface. Specifically, it is possible to explore state-of-the-art SAM combinations that could enhance the device efficiency of inverted PSCs beyond that of silicon solar cells.

*Corresponding author. Email: deyingluo@163.com
© 2024 Chinese Physical Society and IOP Publishing Ltd

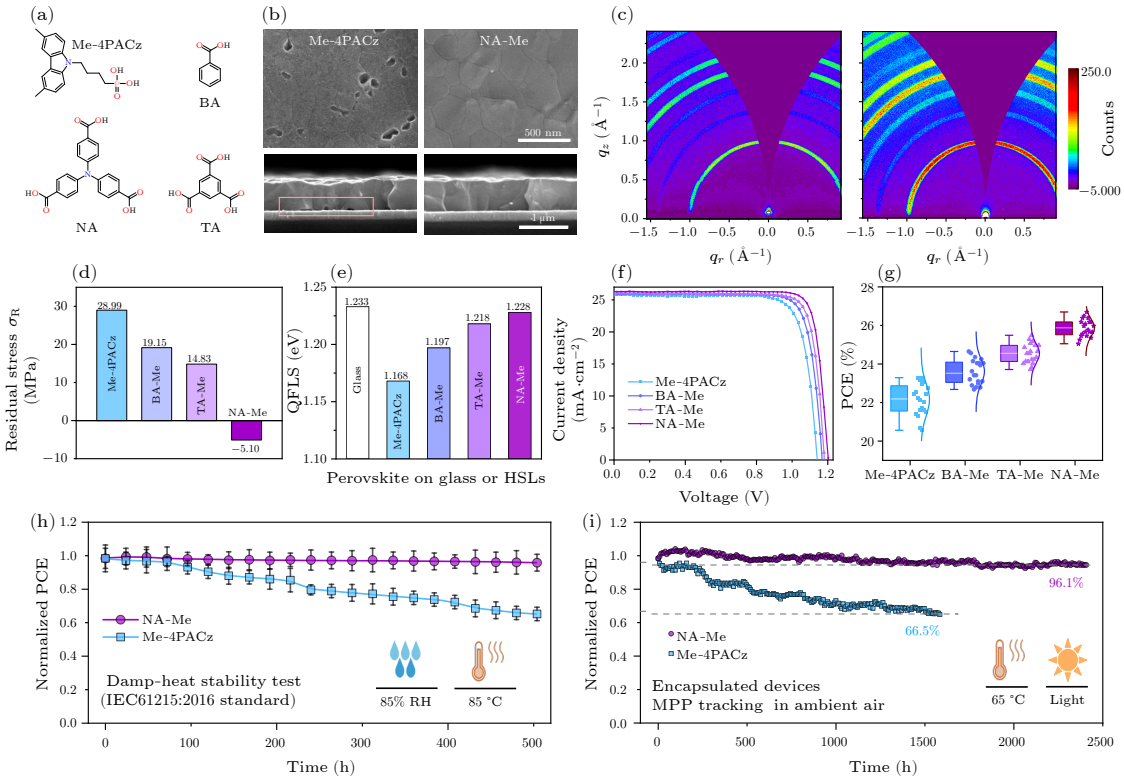

Fig. 1. (a) Molecular structures of Me-4PACz and BA, NA, and TA. (b) Scanning electron microscope (SEM) images of the bottom surface of perovskite films on regular SAM (left) and molecular hybrid substrates (right). (c) Two-dimensional GIWAXS patterns of perovskite films deposited on regular SAM (left) and molecular hybrid substrates (right). The color bar represents the diffraction intensity collected from the GIWAXS detector. (d) Residual stress of perovskite films on different SAM-deposited substrates. (e) The calculated QFLS of perovskite films on glass and different SAM-deposited substrates. (f) *J*–*V* curves of PSCs with different SAMs under reverse scans. (g) Statistics of PCE of inverted PSCs with different SAMs (20 devices). (h) Normalized PCEs of encapsulated devices aged under damp heat conditions (85 ℃ and 85%RH) following the IEC61215:2016 standard. The initial PCEs of regular SAM and molecular hybrid devices used for the damp heat tests are 22.68% and 26.15%, respectively. (i) Operational stability of encapsulated devices under continuous 1-sun equivalent white-light light-emitting-diode illumination with maximum power point tracking in ambient air. The initial PCEs of the regular SAM and the molecular hybrid PSCs used for the operational stability tests are 22.75% and 26.21%, respectively. Taken from Ref. [12].

References

[1] Zhang W, Guo X, Cui Z, Yuan H, Li Y, Li W, Li X, and Fang J 2024 *Adv. Mater.* **36** 2311025
[2] Zhu R 2020 *Nat. Energy* **5** 123
[3] Jiang Q and Zhu K 2024 *Nat. Rev. Mater.* **9** 399
[4] Luo D, Yang W, Wang Z, Sadhanala A, Hu Q, Su R, Shivanna R, Trindade G F, Watts J F, Xu Z, Liu T, Chen K, Ye F, Wu P, Zhao L, Wu J, Tu Y, Zhang Y, Yang X, Zhang W, Friend R H, Gong Q, Snaith H J, and Zhu R 2018 *Science* **360** 1442
[5] Chen P, Xiao Y, Hu J, Li S, Luo D, Su R, Caprioglio P, Kaienburg P, Jia X, Chen N, Wu J, Sui Y, Tang P, Yan H, Huang T, Yu M, Li Q, Zhao L, Hou C H, You Y W, Shyue J J, Wang D, Li X, Zhao Q, Gong Q, Lu Z H, Snaith H J, and Zhu R 2024 *Nature* **625** 516
[6] Luo D, Su R, Zhang W, Gong Q, and Zhu R 2020 *Nat. Rev. Mater.* **5** 44
[7] Zeng J, Bi L, Cheng Y, Xu B, and Jen A K Y 2022 *Nano Res. Energy* **1** 9120004
[8] Yu S, Xiong Z, Zhou H, Zhang Q, Wang Z, Ma F, Qu Z, Zhao Y, Chu X, Zhang X, and You J 2023 *Science* **382** 1399
[9] Peng W, Mao K, Cai F, Meng H, Zhu Z, Li T, Yuan S, Xu Z, Feng X, Xu J, McGehee M D, and Xu J 2023 *Science* **379** 683
[10] Yang X, Luo D, Xiang Y, Zhao L, Anaya M, Shen Y, Wu J, Yang W, Chiang Y H, Tu Y, Su R, Hu Q, Yu H, Shao G, Huang W, Russell T P, Gong Q, Stranks S D, Zhang W, and Zhu R 2021 *Adv. Mater.* **33** 2006435
[11] Zhang S, Ye F, Wang X, Chen R, Zhang H, Zhan L, Jiang X, Li Y, Ji X, Liu S, Yu M, Yu F, Zhang Y, Wu R, Liu Z, Ning Z, Neher D, Han L, Lin Y, Tian H, Chen W, Stolterfoht M, Zhang L, Zhu W H, and Wu Y 2023 *Science* **380** 404
[12] Liu S, Li J, Xiao W, Chen R, Sun Z, Zhang Y, Lei X, Hu S, Kober-Czerny M, Wang J, Ren F, Zhou Q, Raza H, Gao Y, Ji Y, Li S, Li H, Qiu L, Huang W, Zhao Y, Xu B, Liu Z, Snaith H J, Park N G, and Chen W 2024 *Nature* (accepted)
[13] Park S M, Wei M, Lempesis N, Yu W, Hossain T, Agosta L, Carnevali V, Atapattu H R, Serles P, Eickemeyer F T, Shin H, Vafaie M, Choi D, Darabi K, Jung E D, Yang Y, Kim D B, Zakeeruddin S M, Chen B, Amassian A, Filleter T, Kanatzidis M G, Graham K R, Xiao L, Rothlisberger U, Grätzel M, and Sargent E H 2023 *Nature* **624** 289
[14] Xiao Y, Yang X Y, Zhu R, and Snaith H J 2024 *Science* **384** 846
[15] Al-Ashouri A, Köhnen E, Li B, Magomedov A, Hempel H, Caprioglio P, Márquez J A, Morales Vilches A B, Kasparavicius E, Smith J A, Phung N, Menzel D, Grischek M, Kegelmann L, Skroblin D, Gollwitzer C, Malinauskas T, Jošt M, Matič G, Rech B, Schlatmann R, Topič M, Korte L, Abate A, Stannowski B, Neher D, Stolterfoht M, Unold T, Getautis V, and Albrecht S 2020 *Science* **370** 1300